Variability in Frontal Zones in the Southern Ocean along the Greenwich Meridian

William T. B. Billany

Department of Oceanography, University of Cape Town, Rondebosch, South Africa

May 2009

Taught Masters Thesis

Supervisors: Professor Chris Reason & Doctor Juliet Hermes

Contents

List of Figures

List of Tables

Acronyms

ACC – Antarctic Circumpolar Current

AMSR-E - Advanced Microwave Scanning Radiometer – EOS

APF – Antarctic Polar Front

APZ – Antarctic Polar Zone

COADS – Comprehensive Ocean-Atmosphere Data Set

ENSO – El Niño–Southern Oscillation

GRACE - Gravity Recovery And Climate Experiment

GODAE – Global Ocean Data Assimilation Experiment

MADT – Mean Absolute Dynamic Topography

MEI – Multivariate El Niño–Southern Oscillation Index

MOC – Meridional Overturning Circulation

MSLP – Mean Sea Level Pressure

SACCF – Southern Antarctic Circumpolar Current Front

SACCZ – Southern Antarctic Circumpolar Current Zone

SAF – Subantarctic Front

SAM – Southern Annular Mode

SAO – Semiannual Oscillation

SASW – Subantarctic Surface Water

SAZ – Subantarctic Zone

SBdy – Southern Boundary of the Antarctic Circumpolar Front

SBZ – Southern Boundary Zone

SLP – Sea Level Pressure

SST – Sea Surface Temperature

SSH – Sea Surface Height

STF – Subtropical Front

TMI - Microwave Imager

TRMM - Tropical Rainfall Measuring Mission

Abstract

Maps of Mean Absolute Dynamic Topography (MADT) derived from satellite altimetry, for the period January 1993 to December 2007 were used to investigate the variability of the Antarctic Circumpolar Current (ACC) meridional frontal positions and gradients along the Greenwich Meridian. Using the MADT derived meridional frontal positions, the meridional zones between the fronts have been classified. With the classification of the zones established, integrated Sea Surface Temperature (SST) has been used to consider the surface variability in the ACC along the Greenwich Meridian. A strong relationship between the meridional position of the fronts and gradients of MADT exists. In addition, the study found that the meridional positions and gradients of MADT exhibit interannual variability as well as considerable trends over the 15-year time-series. The meridional zones along the Greenwich Meridian also displayed clear trends over the period from June 2002 – November 2007 in integrated SST. The trends suggest a warming and shift in the climate state driving some of the variability in the ACC, which is consistent with other scientific studies. However, the study failed to find convincing correlations with the remotely sensed data used, and the Southern Annular Mode (SAM) on interannual timescales, suggesting that the ACC fronts do not strongly respond to the SAM on interannual time-scales.

1. Introduction

Persistent eastward flow in both the ocean and atmosphere exist in the Southern Hemisphere (Hall & Visbeck, 2002). The strong zonal flow is driven by the large density differences from the equator to pole. The ACC represents the Oceanic component of the zonal flow, which is further enhanced by the westerly winds between 45° – 55°S (Trenberth *et al.* 1990). The westerly winds are associated with the phase of the main mode of atmospheric variability in the Southern Hemisphere, the SAM (Thompson & Wallace, 2000). In recent decades the SAM has favoured a positive phase (Thompson & Solomon, 2002). This raises the possibility that changes in the SAM might be changing the ACC.

The ACC is unique in that it is the only current system that connects each of the ocean basins, and thus an important component of the climate system. It is the primary means by which interocean exchanges of water, heat and salt can occur. These exchanges form an integral part of the Meridional Overturning Circulation (MOC) (Gordon, 1986; Rintoul, 1991; White & Peterson, 1996; Sloyan & Rintoul, 2001a; Sloyan & Rintoul, 2001b; Speich *et al.* 2001). Despite the global importance of the ACC, the Southern Ocean remains relatively poorly sampled due to its remoteness and harsh environmental conditions. Therefore, hydrographic observations remain scarce in both space and time, which means that our understanding of the physical and dynamic processes that contribute to the variability in the Southern Hemisphere climate remain poor.

The ACC is located between the subtropical regimes to the north and the subpolar regimes to the south. Distinct meridional differences in upper ocean water properties mark the boundary between the warmer saltier waters of the subtropics and the

cooler fresher waters of the Southern Ocean (Orsi *et al.* 1995). This boundary is known as the Subtropical Front (STF), and marks the northern extent of the ACC. This front is interrupted by only the South American continent, otherwise the STF marks a continuous boundary around the globe, marking the northern most extent of the Subantarcitc Surface Water (SASW) (Orsi *et al.* 1995). The SASW is cooler and fresher than the warm and more saline subtropical surface waters north of the STF. SASW converges with the subtropical surface waters at the STF and density differences between SASW and subtropical surface water cause the SASW to subduct below the subtropical surface waters (Burls & Reason, 2006). The STF although persistent round most of the Southern Ocean, becomes weak and intermittent in the eastern South Atlantic (Burls & Reason, 2006). An uninterrupted and strengthened STF manifests itself at ~10°E and continues to ~70°E due to the retroflection of the Agulhas Return Current (Lutjeharms & Valentine, 1988; Lutejharms & Ansorge, 2001). The Agulhas Current is the strongest western boundary current in the Southern Hemisphere (Reason, 2001). The Agulhas Current Retroflection region is an area of extreme dynamic variability and it is here that mesoscale eddies are spawned (Lutjeharms & Valentine, 1988). The eddies, otherwise known as Agulhas Rings, perform a critical process whereby heat and salt is exchanged from the Indian Ocean to the South Atlantic Ocean (Lutejharms & Ansorge, 2001). In addition, the Agulhas Rings can propagate south of the STF transporting heat and salt into the northern limb of the ACC (Swart *et al.* 2008). Baroclinic transports have the greatest variability north of ~42.5°S in the South Atlantic sector of the ACC due to the meridional stability of the STF and the presence of Agulhas Rings (Swart *et al.* 2008).

The ACC is convergent in nature (Belkin & Gordon, 1996), deep water upwells, and is transported northward in an Ekman layer, and then sinks at the Antarctic Convergence (Speer *et al.* 2000), otherwise known as the Antarctic Polar Front (APF) (Moore *et al.* 1997, 1999). To compensate for this northward flow of intermediate and bottom water, the deep waters propagate southward toward the Antarctic shelf (Speer *et al.* 2000). Classically the ACC is regarded as having three convergent fronts (Orsi *et al.* 1995). These three fronts extend from the ocean surface to the deep ocean: from north to south, the three fronts are the Subantarctic Front (SAF), the APF, and the Southern ACC Front (SACCF) (Orsi *et al.* 1995; Sokolov & Rintoul, 2007). The Southern Boundary of the ACC (SBdy) separates the ACC from the subpolar gyres (Orsi *et al.* 1995). Weak convergence of the Southern Boundary Zone (SBZ) waters and subpolar gyre waters has made this boundary difficult to define. The SBdy exists due to the southward divergent flow of the SBZ. The SBZ is a zone of water in the ACC, its boundaries are defined by the location of the SACCF (northern boundary) and the SBdy (southern boundary) (Swart *et al.* 2008).

The dominant mode of variability in the extratropical Southern Hemisphere is the SAM (Thompson & Wallace, 2000; Hall & Visbeck, 2002; Thompson & Solomon, 2002; Marshall, 2003; Sen Gupta & England, 2006). Like the Southern Ocean, the atmosphere in the Southern Hemisphere is uninhibited by topographic features at the midlatitudes. This allows a strengthened westerly atmospheric jet to circumnavigate the Southern Hemisphere (Hall & Visbeck, 2002). Although the SAM is highly zonally symmetric in its spatial structure (Thompson & Wallace, 2000; Marshall, 2003), it is known to exhibit a wavenumber 3 structure with the three centres located over the three southern subtropical ocean basins (Mo, 2000). The SAM is seen to have an

oscillating structure over time, a positive and negative phase. Oscillating on all temporal scales from the synoptic to centennial (Hall & Visbeck, 2002). During a positive (negative) phase the westerly surface winds increase (decrease) with zonal symmetry across the Southern Hemisphere (Hall & Visbeck, 2002). A positive (negative) phase of the SAM is characterised by an extension (contraction) of the subtropical high pressure systems and an intensification (abatement) of the subpolar low pressure cells in the Southern Hemisphere. This seesaw motion of tropospheric mass is an indicator of the meridional position of the westerly storm track (Gong & Wang, 1999).

Hall & Visbeck (2002) found that theoretically there should be a degree of co-variability between the SAM and the Southern Ocean. In the circumpolar ocean region the westerly winds prevail, driving a northward Ekman drift within the ACC. Northward flow within the ACC creates divergent flow in the surface waters of the ACC away from the Antarctic continent. This northward flow of cold divergent water prevents the warm subtropical waters from reaching Antarctica. As warm waters are kept away from the high latitudes in the Southern Hemisphere the density gradient is further enhanced. The density gradient created effectively generates the strong eastward flow of the ACC. Furthermore, the westerly winds track across different latitudes over the Southern Ocean and in doing so, waters within the Ekman layer move north and south depending on the meridional location of the westerly winds. The southward and northward moving waters converge and diverge, creating frontal regions and divergent zones within the ACC.

If the ACC is influenced by the atmospheric forcing on the ocean, and the main mode of variability in the atmosphere in the Southern Hemisphere is the SAM. It is likely

that the SAM will influence the variability within the ACC. Models suggest that it is likely that the SAM is responsible for at least part of the variability in the ACC (Hall & Visbeck, 2002; Sen Gupta & England, 2006). Observational evidence, however, is not as well documented. Cai (2006) attributed the more southward advection of the subtropical water to a southward shift in the westerly winds. Sallée *et al.* (2008) found that the ACC responds to changes in the westerly winds and the phase of the SAM. Interestingly, the changes in the westerly winds are thought to be caused by ozone depletion in the Southern Hemisphere and changes to the SAM (Thompson & Solomon, 2002).

This study used observations from satellite altimetry to locate the ACC frontal positions and describe their associated variability, and in doing so validate whether the frontal positions derived from altimetry data agree with the classic frontal positions found by Orsi *et al.* (1995). The frontal positions found by Orsi *et al.* (1995) were obtained from hydrographic data. Furthermore, this study aims to describe the surface variability of the zones between the fronts of the ACC using integrated SST data.

An attempt was made in this study to investigate if the signal of the SAM and the El Niño–Southern Oscillation (ENSO) is evident in observational data of the ACC at the Greenwich Meridian and if the SAM influences the variability of the fronts as suggested by the Hall & Visbeck (2002) idealised model.

As the ACC is a critical component of the climate system, its features, extent and variability must be understood fully (Orsi *et al.* 1995). This study was limited due to time constraints and was therefore only conducted at a single longitude in the

Southern Ocean. The Greenwich Meridian was chosen, as it is reasonably stable from the downstream perturbations caused by the Drake Passage and far enough to the west to not be influenced dramatically by the flow of Agulhas Current and Agulhas Return Current. Observing the variability of the ACC at a longitude with reduced 'noise' from dominant external forcings allows the lower frequency variability of the ACC to be detected, which is thought to aid the detection of atmospheric signals within the variability of the ACC. Please refer to the topographic map of the Southern Ocean from -60° – 120°E , which can be found in the Appendix.

2. Data

2.1 Satellite Altimetry Data

Maps of MADT were used to describe the variability of the fronts of the ACC at the Greenwich Meridian. MADT is the sum of the sea level anomaly data and mean dynamic topography From Rio & Hernandez (2004). The mean dynamic topography is obtained through a combination of in-situ measurements (hydrographic & surface drifter data), altimetry data and the EIGEN-GRACE 03S geoid. The altimetry products are produced from the combination of four different altimeter instruments on individual satellite platforms: Topex/Poseidon, Jason-1, ERS-1/2 and ENVISAT. The altimetry data is available at weekly time-steps with a spatial resolution of 1/3° and mapped on a Mercator grid. The MADT data are referenced to a seven-year (1993-1999) mean. For further information on mapping techniques and error corrections refer to Le Traon *et al.* (1998), Le Traon & Ogor (1998) and Ducet *et al.* (2000).

2.2 Satellite Sea Surface Temperature Data

To investigate the variability of the zones within the ACC at the Greenwich Meridian the Microwave Optimally Interpolated SST gridded data is used, and is available from

June 2002. The blended Microwave Optimally Interpolated SST product uses data obtained from the Microwave Imager (TMI) onboard the Tropical Rainfall Measuring Mission (TRMM) satellite and is NASA's Advanced Microwave Scanning Radiometer component for the Earth Observing System (EOS) (AMSR-E). The Microwave Optimally Interpolated SST product has a spatial resolution of 1/4° (~25km) and is available daily. Before the data are included in the optimally interpolated analysis they are corrected for errors and biases known in the instruments. Near-real-time validation and bias corrections are undertaken using in-situ data retrieved from the Global Ocean Data Assimilation Experiment (GODAE). Collocation of the TMI AMSR-E data with GODAE data only occurs if the TMI AMSR-E data is taken within 25km and within six hours of in-situ sampling under GODAE. Only after the errors have been determined are the data blended together. The blending is done using the method described by Reynolds & Smith (1994). Coverage of the TMI instrument is limited to a latitudinal band between 40°N and 40°S. The AQUA satellite has a near polar orbit providing the AMSR-E instrument with global coverage. Much of the data used in this study are beyond or at the limit of the TMI instruments range and therefore based mainly on the AMSR-E instrument. Unfortunately the AMSR-E instrument does not have daily global coverage. Furthermore, the mean spatial resolution of the AMSR-E instrument is coarser at ~58km. Nonetheless, the swath gaps and reduced spatial resolution do not pose a serious issue when considering data consolidated in to monthly averages as is the case in this study.

2.3 The Southern Annular Mode & El Niño Southern Oscillation Indexes

The SAM index as described Marshall (2003) has been used in this study. The index is based on station data from six stations at ~40°S and another six stations situated at ~65°S in the Southern Hemisphere.

The proxy zonal Mean Sea Level Pressure (MSLP) at both 40°S and 65°S is calculated. Station derived MSLP is then compared to NCEP-NCAR reanalysis data on 2.5° latitude – longitude grid. This true zonal mean is the mean of 144 points along the appropriate parallel. Data corresponding to station observations were determined by interpolating the NCEP-NCAR reanalysis MSLP fields to the station location to the nearest 0.1°. The difference in MSLP at 40°S and 65°S is how the SAM index is defined. This index was preferred over a purely reanalysis based index as biases in reanalysis constructions in the SAM have been found (Hines *et al.* 2000). Additionally, this study uses observational data and it is therefore deemed appropriate to use an observation corrected SAM index. For further details on the SAM index please refer to Marshall (2003).

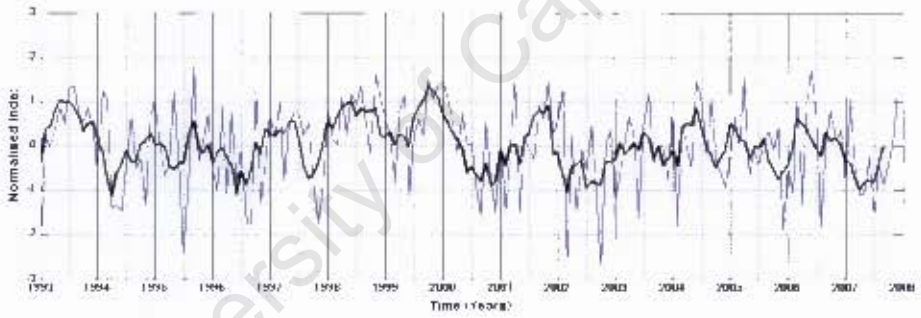

Figure 1. The SAM index (Marshall, 2003). Blue line is the monthly SAM index, the thick black line is an 4-month running mean of the monthly SAM index to identify the lower frequency variability of the SAM.

The Multivariate ENSO Index (MEI) has been used in this study to identify if the ENSO signal is being projected into some of the variability found in the fronts and zones of the ACC at the Greenwich Meridian. The MEI is derived from tropical Pacific Comprehensive Ocean-Atmosphere Data Set (COADS) records (Wolter & Timlin, 1998). The MEI is based on the six main observed variables in the tropical Pacific in an attempt to reduce errors in individual variables. These six variables are: sea-level pressure, zonal and meridional components of the surface wind stress, sea surface

temperature, surface air temperature, and total cloudiness fraction of the sky (Wolter & Timlin, 1993).

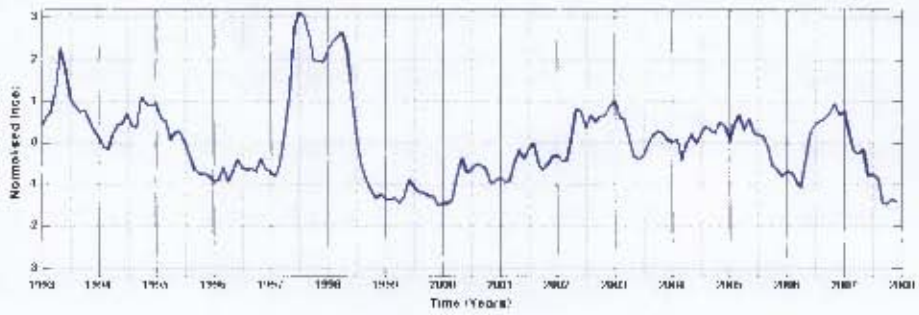

Figure 2. Bimonthly Multivariate El Niño–Southern Oscillation Index (MEI) from January 1993 to December 2007.

3. Meridional Frontal Characteristics and Associated Variability Inferred From Satellite Altimetry

The fronts of the ACC are relatively narrow belts characterised by elevated current velocities, marked horizontal gradients in temperature, salinity, Sea Surface Height (SSH), and other oceanographic properties (Orsi *et al.* 1995; Belkin & Gordon, 1996; Moore *et al.* 1999; Sokolov & Rintoul, 2007. Swart *et al.* 2008). Sokolov & Rintoul (2007) investigated the frontal positions and structures and found that whilst there are five general frontal features, each frontal feature generally consists of multiple branches that merge and diverge along their circumpolar paths. Figure 4 identifies the more complex frontal structure of the ACC along the Greenwich Meridian as a series of pronounced uv velocities. Only the main frontal features of the ACC, identified by the most prominent MADT gradients were classified in this study (see Figure 3).

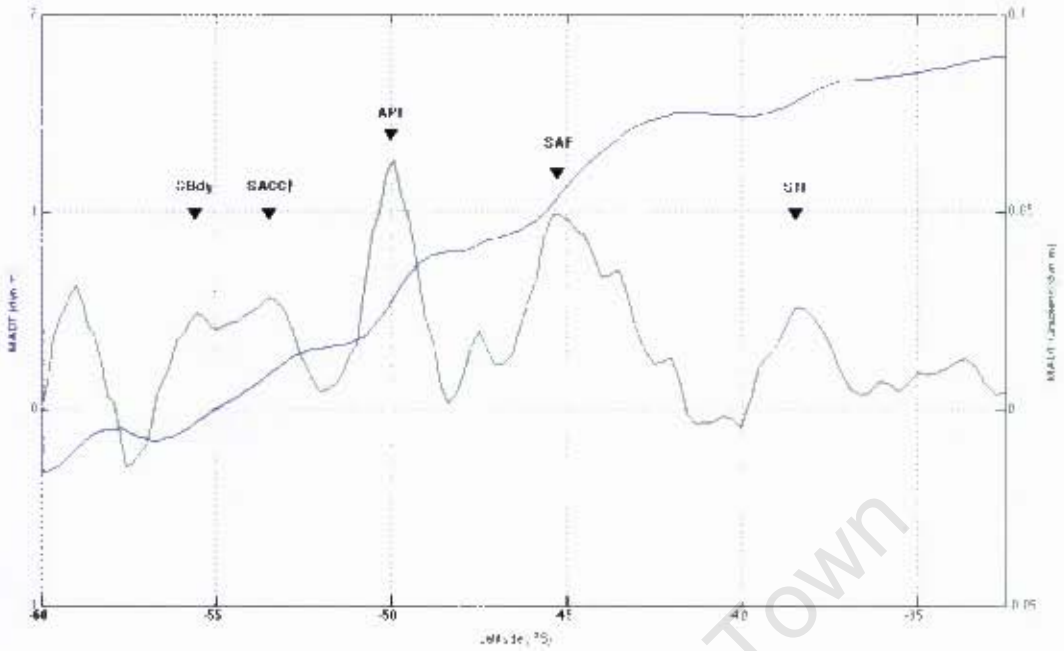

Figure 3. MADT data (dyn m) (solid blue line) and MADT meridional gradient (solid green line) at the Greenwich Meridian. The mean frontal positions of the ACC at the Greenwich Meridian found by the MADT and MADT meridional gradient are marked.

To consider the monthly and interannual variability of the fronts within the ACC the weekly data has been amalgamated into monthly averages for the January 1993 - December 2007 period to remove some of the higher frequency variability. The frontal positions of the ACC at the Greenwich Meridian have been located using the meridional gradient of MADT from the monthly averages. The mean meridional position of the MADT with the highest gradients was found. Using the latitudinal positions of the greatest gradients it is possible to extract the value of MADT for each gradient 'spike' (Figure 1). By following the value of MADT at each time-step and locating the corresponding latitudinal value it is possible to locate the frontal positions of the ACC at the Greenwich Meridian over the period in question. This method proved reasonably robust with mean meridional frontal positions in close agreement with the hydrographic derived frontal positions as defined by Orsi *et al.* (1995) at the Greenwich Meridian (Table 1).

3.1 Meridional Frontal Positions and Associated Variability

To illustrate the meridional interannual variability of the ACC at the Greenwich Meridian, Figure 3 displays the altimetry derived surface velocity magnitude in ms^{-1} at each monthly time step over the January 1993 – December 2007 period. The meridional frontal positions have been plotted over the surface velocity magnitudes ($\sqrt{(u^2 + v^2)}$). Swart and Speich (2009) found that the isolines of MADT closely follow the surface current magnitudes of the main ACC fronts along the GoodHope transect. This study agrees with the findings by Sokolov and Rintoul (2007) and Swart *et al.* (2009) that the MADT isolines do provide an accurate method of locating the meridional frontal positions and that these meridional positions correspond closely with the classic frontal positions found by Orsi *et al.* (1995) (Table 1).

Table 1. Criteria Used to locate the ACC Fronts, reproduced from Orsi *et al.* (1995)

Front	Criteria	Classical Position (°S)	MADT Derived Mean Frontal Position (°S)	Frontal Position Standard Deviation
STF	$10°C < \theta_{100T} < 12°C$	38.4	38.5	0.79
SAF	S < 34.20 at Z < 300m θ > 4 5°C at 400m	45.7	45.3	0.31
APF	θ < 2°C along θ_{min} at Z < 200m	49.4	50.0	0.27
SACCF	θ > 0°C along θ_{min} at Z < 150m	52.4	53.5	0.19
SBdy	Southern limit of vertical maximum of θ > 1.5°C, (~200m)	56.1	55.6	0.28

The fronts in the table are as follows: Subtropical Front (STF), Subantarctic Front (SAF), Antarctic Polar Front (APF), Southern ACC Front (SACCF), Southern Boundary of the ACC (SBdy). θ is the potential temperature, S is the Salinity. The classical positions are for the Greenwich Meridian, as determined by Orsi *et al.* (1995). The MADT derived mean frontal position and associated standard deviation for each front are listed.

The GoodHope cruise track, which was first established in early 2004 (http://www.ifremer.fr/lpo/speich/GOODHOPE/goodhope.htm) crosses the STF at approximately 40.5°S and 10°E. Swart *et al.* (2008) found that the MADT could not realistically capture the STF at this location due to the intense mesoscale activity caused by the propagation of Agulhas Rings in the region. Unlike the GoodHope transect, this study focused on the STF at the Greenwich Meridian. Here the STF is less influenced by Agulhas Rings, in comparison to the STF at the GoodHope transect further to the east, which encounters Agulhas Rings on the order of ~2 per year (Swart *et al.* In Press). Nonetheless, the STF remains the most variable of fronts within the ACC at the Greenwich Meridian with the greatest meridional standard deviation (± 0.79° latitude). When not influenced by mesoscale eddies the MADT contour used for the STF follows the velocity magnitudes reasonably well. The SACCF showed the least meridional variability of all the fronts of the ACC at the Greenwich Meridian (± 0.19°).

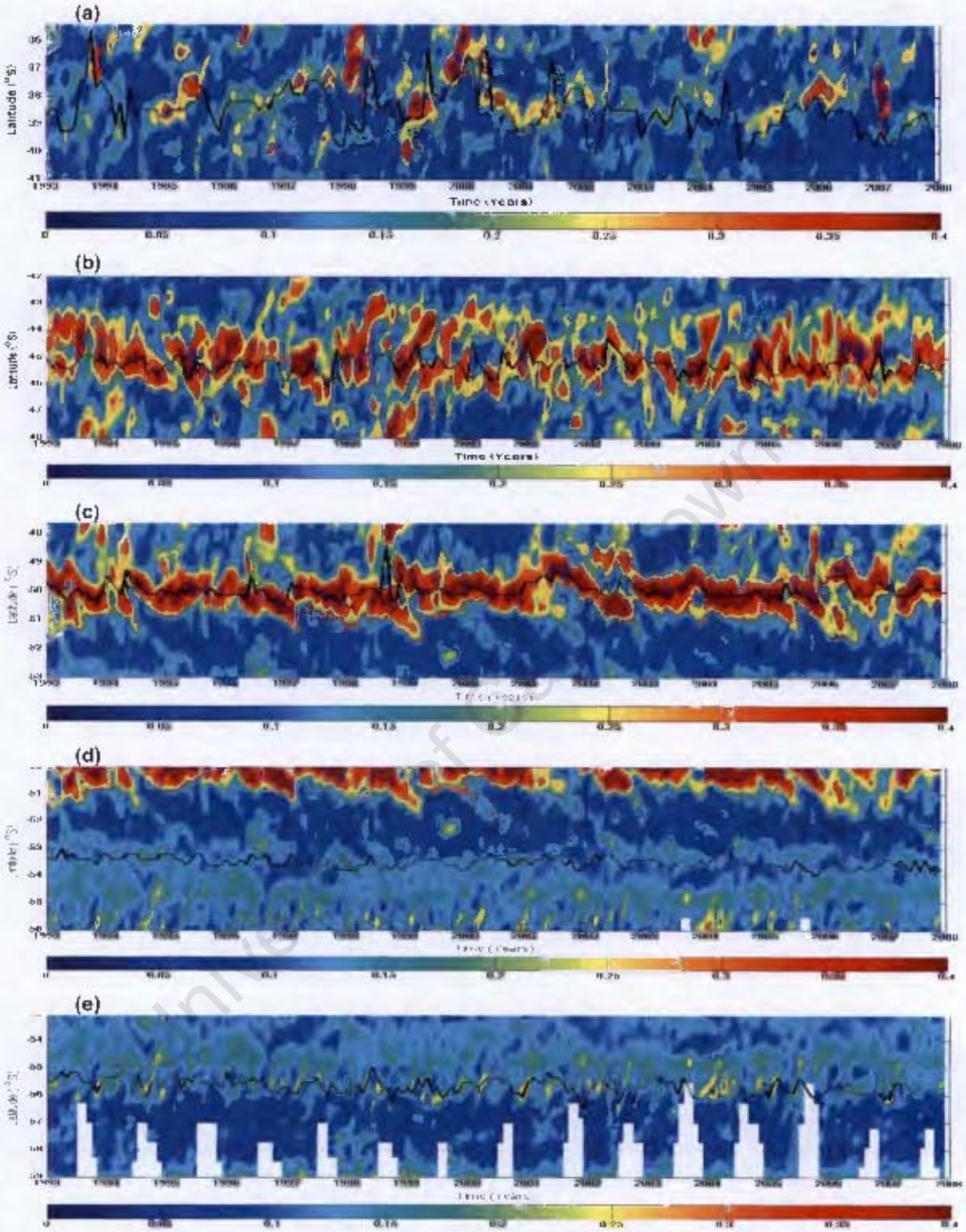

Figure 4. Collection of Hovmöller plots of UV velocity magnitudes (colour surface plot; in ms^{-1}) and MADT derived frontal positions of the ACC (black lines; in dyn m) along the Greenwich Meridian from January 1993 to December 2007. This is illustrated for (a) The STF, (b) the SAF, (c) the APF, (d) the SACCF, (e) the SBdy.

The MADT isolines for the fronts are shown in Figure 4, from north to south the fronts are as follows: (a) STF = 1.56 dyn m (1 dyn m = $10 m^2 s^{-2}$), (b) SAF = 1.09 dyn m, (c) APF = 0.58 dyn m, (d) SACCF = 0.19 dyn m, (e) SBdy = -0.06 dyn m. It is clear from both Figure 3 and Figure 4b and c that both the SAF and APF are particularly well defined when using MADT. The main branch of the SAF is chosen in this study, however, it is clear to see that there is often another northern frontal feature of the SAF, which is found at approximately 44° – 43°S (Figure 4b). This is also clearly identifiable in Figure 3 (Moore *et al.* 1999; Sokolov & Rintoul, 2007). The APF is a distinct front and does not appear to have any other branches or filaments associated with it at the Greenwich Meridian (see gradient of MADT in Figure 3). The boundary separating the SACCF and SBdy are more difficult to distinguish in Figure 4d and e. This is due to the relatively small change in gradient between the SACCF and SBdy, as can be identified in Figure 3.

Anomalous uv velocity magnitudes are apparent in close proximity to the STF along the Greenwich Meridian (Figure 4a). Displayed are four events of high uv velocity magnitudes, which appear in the following chronological order: September – November 1993, February – March 1998, and May 1999 – May 2000, and January – March 2007. These mesoscale structures are persistent over monthly timescales. Excluding the uv velocity magnitude anomaly in early 2007, the anomalies are associated with the STF meridional position being incorrectly identified. Further investigation reveals the errors in frontal position of the STF are associated with mesoscale eddy activity in the vicinity of the STF, along the Greenwich Meridian. Figure 5 displays weekly snapshots of MADT data of an anomalous event in during 1999/2000. The snapshots allow individual mesoscale eddies to be indentified and followed through time. The close proximity of eddies causes the value of MADT to

move northward away from the meridional position of the STF at the Greenwich Meridian toward the track of eddies (Figure 5b to d) that are often referred to as the Agulhas Corridor (Witter & Gordon, 1999). During August 1999 a train of eddies shed from the Agulhas Current cross the Greenwich Meridian near to the STF. Since Agulhas Rings are anticyclonic they are readily identified by altimeter observations as they display a positive sea level anomaly relative to surrounding ocean environment (Witter & Gordon, 1999). This explains why the value of MADT used for following the STF through time (1.56 dyn m) is also found in the eddy passing the Greenwich Meridian in August 1999. The northward migration in the value of MADT continues through to April 2000, trailing a mesoscale eddy moving in a northwest direction. By April 2000 the mesoscale feature is no longer present along the Greenwich Meridian. Also, the amplitude of the mesoscale eddy signature has decayed to a point where the value of MADT used to find the STF frontal position is no longer found in proximity to the mesoscale eddy. The value of MADT is again located southward in April 2000 at 38.5°S, which is 0.01° from the latitudinal mean of the STF at the Greenwich Meridian. In June 2000 (Figure 5f) another eddy causes the MADT value used to follow the STF, to shift northward, again due to another mesoscale eddy. Continual eddy disturbances occur during the 1993, 1998 and 1999/2000 periods at the Greenwich Meridian.

The isoline used to follow the APF was found to mistakenly identify the APF on one occasion in late 1998. The errors have been included in Figure 4, to show how the contour lines will follow the uv velocity magnitudes and eddy activity. However, errors associated in the frontal positions due to incorrectly tracking of fronts have been removed from all further Figures and analysis from this point.

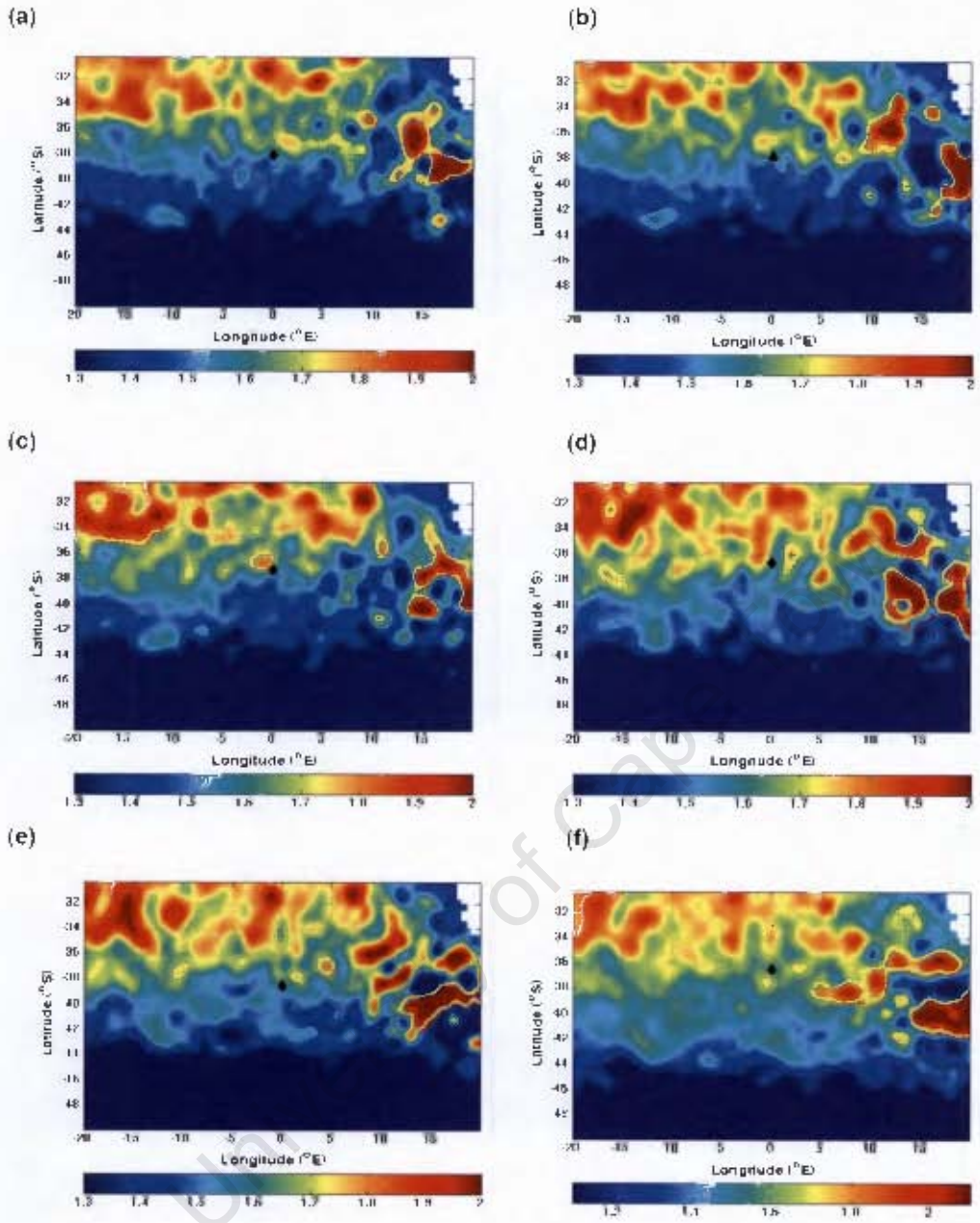

Figure 5. Bimonthly snapshots of MADT (dyn m) in a region located at and near the Greenwich Meridian and STF meridional position (black diamond), which was found following a contour of MADT through time. The bimonthly snapshots of the first week of each month were taken in the following order: (a) August 1999, (b) October 1999, (c) December 1999, (d) February 2000, (e) April 2000, (f) June 2000.

3.2 Seasonal Variability in the Meridional Positions and Gradients of MADT in the Fronts of the ACC at the Greenwich Meridian

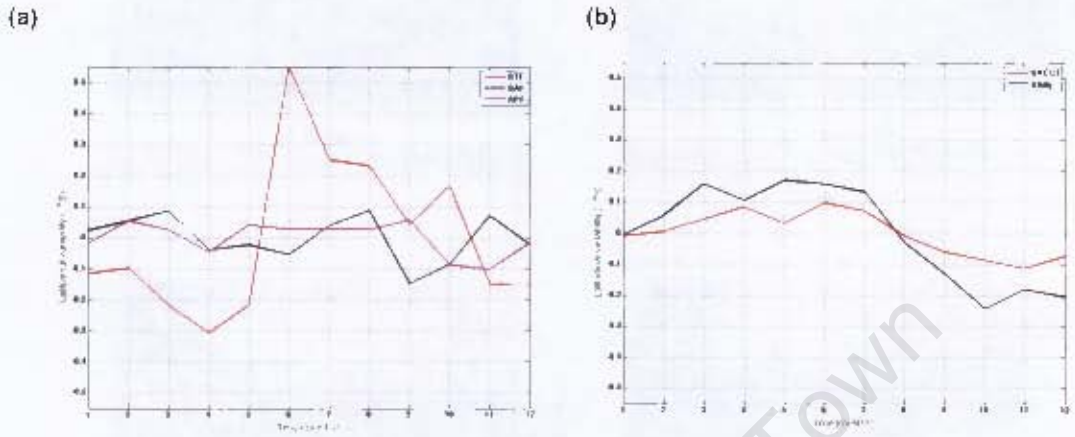

Figure 6. Mean seasonal meridional shifts (° latitude) in the frontal positions in the ACC at the Greenwich Meridian from a 15-year continuous time-series. The fronts were split in to two latitudinal groups, as different characteristics are likely to be identified in the two groups (Van Loon, 1967). (a) The ACC fronts north of 50°S: STF (thick red line), SAF (thick black line), APF (thick magenta line). (b) The fronts of the ACC south of 50°S: SACCF (thick red line), SBdy (thick black line).

The seasonal changes in the Southern Ocean are known to play a part in the variability in a number of atmospheric and oceanic components (Rouault *et al.* 2005). Here the study explored the seasonal variability of the meridional positions and gradient of MADT in the ACC fronts. Figure 6a plots the mean meridional seasonal variability of the fronts at and north of 50°S of the ACC at the Greenwich Meridian. Seasonal variability in both the SAF and APF are not particularly strong at any month. The STF however, does appear to have a more pronounced mean seasonal cycle. A rapid change in the meridional frontal position occurs April (38.8°S) to its most northern position in June (37.9°S). The northern most location of the STF in June agrees with Meehl (1991) that the ocean heat storage in the Southern Ocean is at its minimum in June. From June the STF migrates back towards its most southerly location (April) at a slower rate. In October and February there appear to be small

northward shifts in the mean meridional seasonal frontal position of the STF. The more pronounced seasonal variability is likely due to the fact that the STF at the Greenwich Meridian marks the upper ocean boundary between the Southern Ocean and subtropical gyre of the South Atlantic. The southern fronts follow a more sinusoidal nature and as expected venture in the north (south) during austral winter (summer) (Figure 6b).

(a) (b)

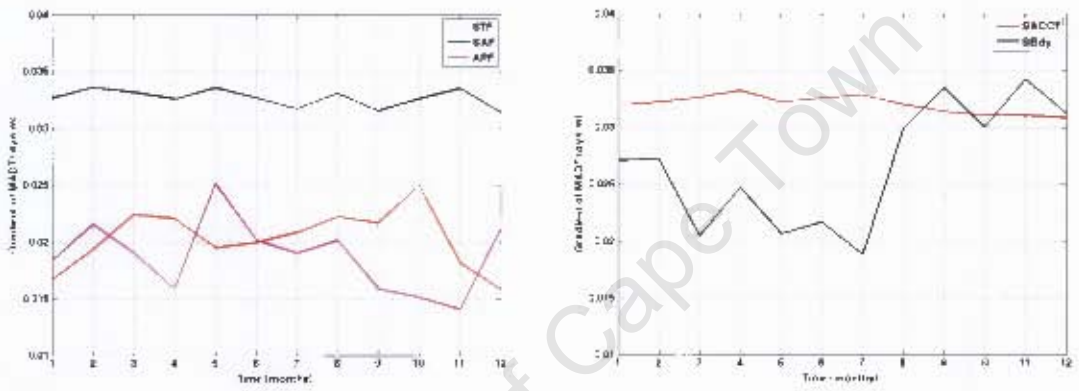

Figure 7. Mean season variability in the gradients (dyn m) of the fronts in the ACC at the Greenwich Meridian from a 15-year continuous time-series. (a) The ACC fronts north of 50°S: STF (thick red line), SAF (thick black line), APF (thick magenta line). (b) The ACC fronts south of 50°S: SACCF (thick red line), SBdy (thick black line).

Mean seasonal variations in the gradient of MADT of the STF show a semiannual cycle (see Figure 7a). There are two peaks in the MADT gradient of the STF, one in April (0.0221 dyn m), and the second in October (0.0250 dyn m), the troughs in this semiannual cycle occur in May (0.0195 dyn m) and December (0.0158 dyn m). The two peaks in the MADT gradient of the STF coincide with southward migrations in the meridional frontal position of the STF. Furthermore, the most northward mean meridional seasonal position of the STF occurs in June, when the MADT gradient monthly mean value is relatively weak (0.0200 dyn m). The second trough in the MADT gradient of the STF occurs in January, the meridional seasonal position in

January and February is located in a slight northward migration. Unlike the period in June however, during January the surface waters of the Southern Ocean are experiencing warming as it is the austral summer. This may help explain the northward extension of the STF in June. A decrease in the gradient of MADT favours northward migrations in the meridional frontal position of the STF, which during June is likely to be further north as this is during the austral winter. During the austral winter the position of the STF migrates further north due to a cooling of the upper ocean waters.

The seasonal variability of the meridional position and gradient of MADT in the SAF both display weak seasonal cycles. Furthermore, the peaks and troughs of the SAF in the meridional position and gradient of MADT are in close agreement. In fact, when comparing Figure 6 and 7 the SAF, APF and SACCF all show mean seasonal shifts northward in their meridional frontal positions during months more prevalent to stronger gradients and vice versa. Yet the boundaries of the ACC, the STF and SBdy share similar mean seasonal responses to their gradient of MADT and their meridional positions. Nevertheless, the seasonal cycles do differ. This is not surprising as the boundaries are situated at either latitudinal boundary of the ACC and it is therefore likely that they are influenced differently by seasonal changes. The SBdy shows a smoother more predictable mean annual cycle in both its gradient of MADT and meridional position (Figure 6b & 7b) than the STF, which shows a semi-annual cycle in its gradient of MADT and a more abrupt northward meridional shift during the peak of winter (Figure 6a & 7a).

3.3 Interannual variability of fronts at the Greenwich Meridian using altimetry

To better capture the lower frequencies of variability in meridional positions and gradient, the mean seasonal variability has been removed. Seasonal variations in the frontal positions are not considered the dominant mode of variability, nevertheless, there is a seasonal component to both the gradient of MADT and altimeter derived meridional positions. What is more, there is a relationship between the gradient of MADT and meridional position of the fronts within the ACC when considering the mean seasonal variability of the fronts within the ACC at the Greenwich Meridian. Despite this, it must be stressed that the variability in the gradient of MADT is not driving the meridional position of the fronts or the other way around. It is likely that response in the gradient of MADT and the meridional position are both driven simultaneously by other forcings. To further explore this, the relationship between the interannual variability of meridional frontal positions and the gradient of MADT (see Figure 8) throughout the entire 15-year time-series will be considered.

Caution must be exercised when interpreting the results of the STF prior to 2002, which do not appear to be strongly out of phase when the inaccurate features have been removed (Figure 8a). Before 2002 Agulhas Rings were found to disturb the MADT contour being used to follow the STF. The three main fronts within the ACC show persistent positive relationships in their meridional positions and gradients of MADT (see Table 2).

Table 2. Monthly timeseries correlations of the meridional positions and gradients of MADT of the fronts within the ACC at the Greenwich Meridian

Frontal Position	Gradient (r value)
STF	0.28
SAF	0.51
APF	0.94
SACCF	0.96
SBdy	-0.63

Correlations were based on the normalised index of both variables with mean seasonal variability and mesoscale associated errors removed. The significance for all r values in Table 2 are greater than the 99% confidence level.

Five northward extensions in the meridional positions of the SAF are also marked by considerable 'spikes' in the gradient of MADT (Figure 8b). The five spikes occur chronologically as follows: January – February 1999, January 2000, June – July 2000, January 2001, and March – April 2002.

One event occurs in the corrected APF position and gradient of MADT where a negative relationship between the meridional position and the gradient of MADT is observed. In December 1996 there is a southward shift in the APF, its most southerly migration in the entire time-series, which coincides with a slight positive value in the gradient of MADT. Otherwise, the APF meridional position follows the gradient changes in strength exceptionally well (Table 2).

There is a strong positive relationship (r=0.96) between the meridional position and gradient of MADT of the SACCF. Northward migrations in meridional position of the SACCF are associated with an increase in the gradient of MADT. There appears to be a negative trend in the meridional position and strength of the SACCF over the 15-

year time-series. A period of stability in meridional position and gradient of MADT occurs from 2000 to 2004, before the negative trend again becomes apparent. The SBdy displays a negative relationship in its meridional position and gradient of MADT, except during an extended period from mid 2001 to late 2002 when there is a positive correlation, otherwise, the negative correlation is strong (see Table 2).

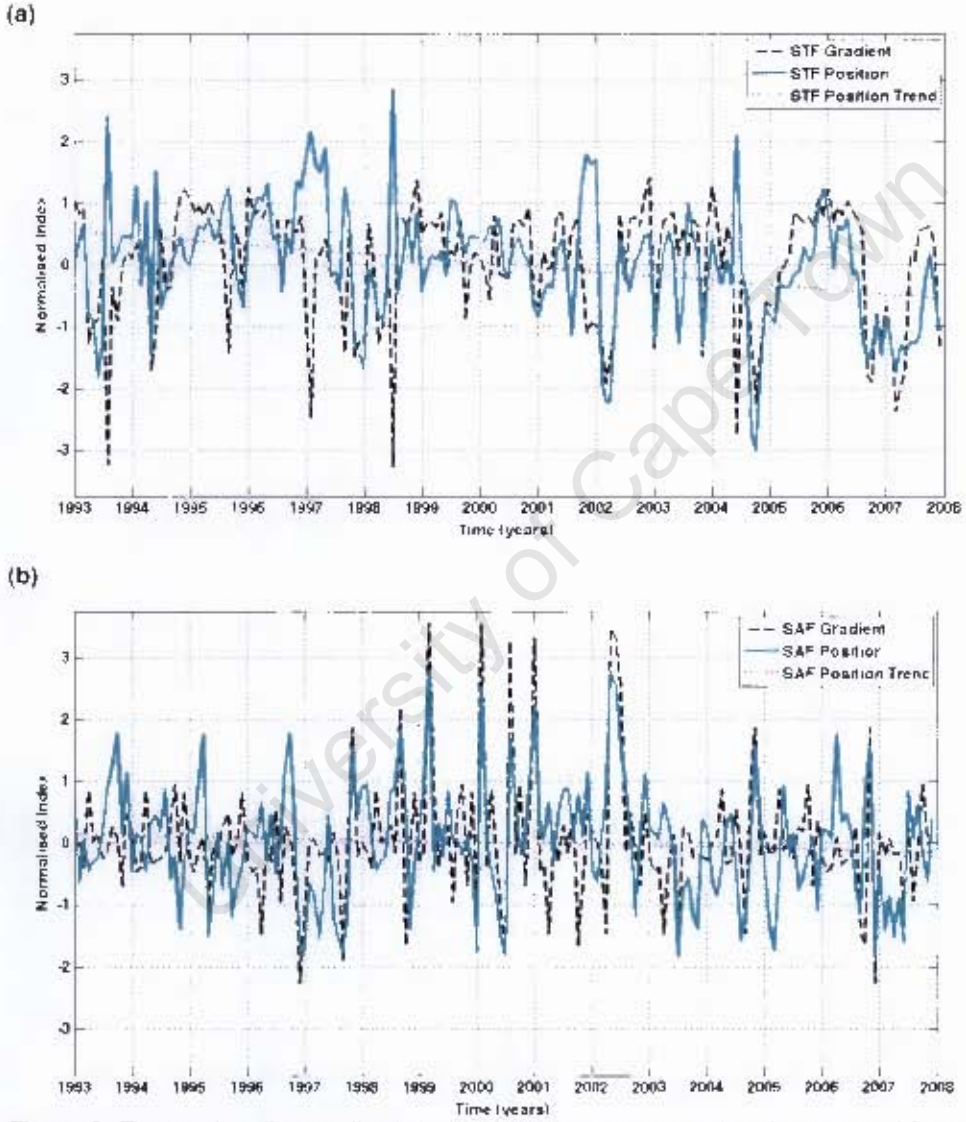

Figure 8. Time-series of normalised data with the mean seasonal cycles removed from the meridional frontal positions (thick cyan line), gradient of MADT of the fronts (black dashed line) plotted with the frontal position trend line (blue dotted line). A 5-month running mean has been applied to all the data to highlight periods of extended anomalous behavior and remove the higher frequency intra-monthly variability. This is illustrated for (a) The STF, (b) the SAF, (c) the APF, (d) the SACCF, (e) the SBdy. The inaccurate gradient values of MADT and positions in the fronts have been removed.

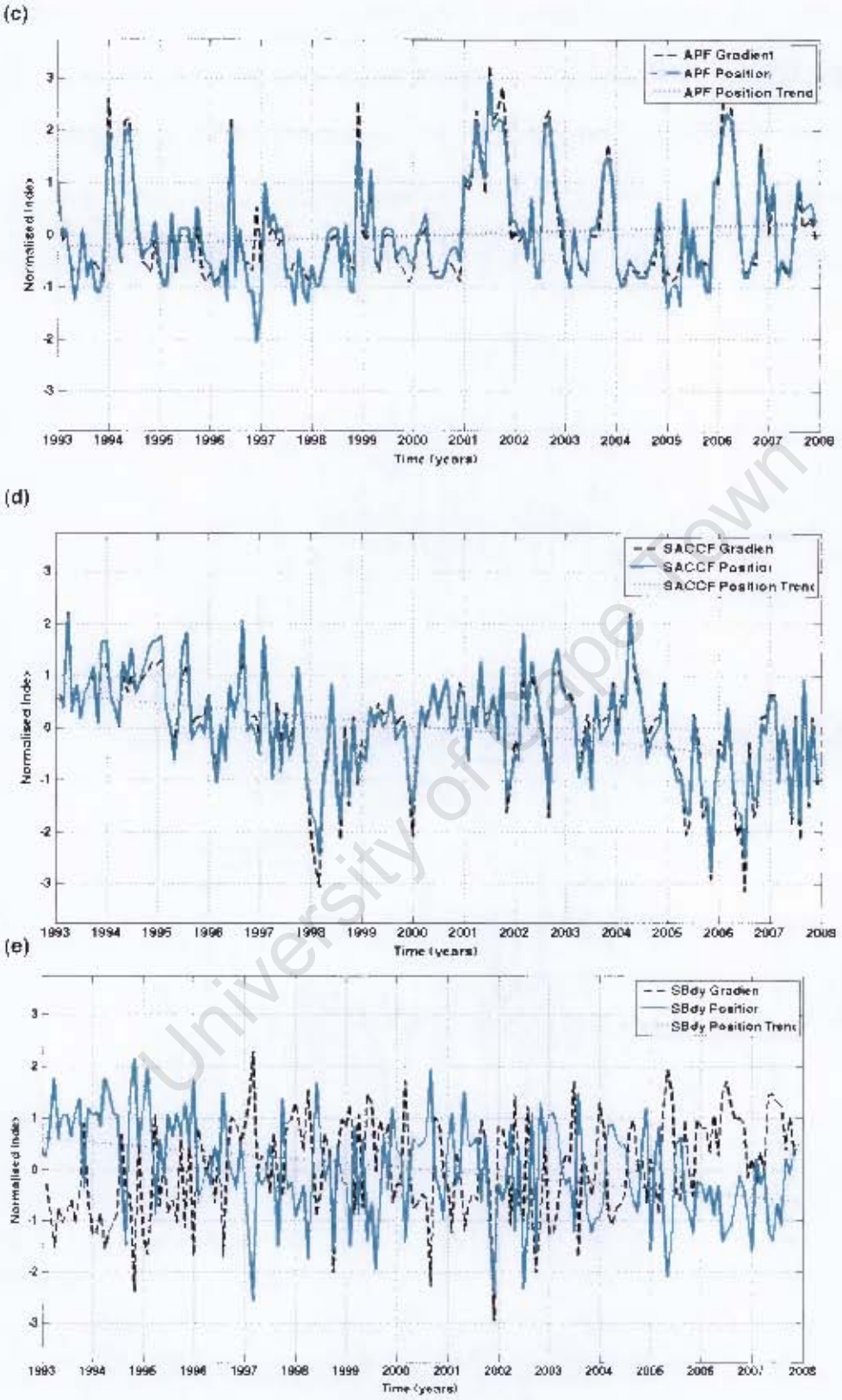

Figure 8. Time-series of normalised data with the mean seasonal cycles removed from the meridional frontal positions (thick cyan line), gradient of MADT of the fronts (black dashed line) plotted with the frontal position trend line (blue dotted line). A 5-month running mean has been applied to all the data to highlight periods of extended anomalous behavior and remove the higher frequency intra-monthly

variability. This is illustrated for (a) The STF, (b) the SAF, (c) the APF, (d) the SACCF, (e) the SBdy. The inaccurate gradient values of MADT and positions in the fronts have been removed.

3.4 Atmospheric modes and the fronts of the ACC at the Greenwich Meridian

The monthly SAM index was superimposed over the normalised frontal gradients of MADT and their meridional positions to identify any possible relationship. The normalised position of the STF showed a positive correlation with the SAM, when applying a 5-month running mean ($r = 0.32$ not significant above 95%) and when correlating the monthly data ($r = 0.16$ not significant above 95%). Despite the positive correlation with the SAM and the meridional position of the STF, the corrections in the meridional position of the STF may bias some of the results. The anomalous events in the STF, which were removed, occur during positive phases in the SAM (see Figure 4a). Correlation of the STF with the SAM without correcting the frontal position of the STF resulted in an r-value of 0.45 (significant above 99%), this is found with a 5-month running mean is passed through the data. The 5-month running mean also highlights the in phase relationship of the meridional position and gradient of MADT in the STF after 2002. During this in phase relationship the SAM leads both the position and gradient of the STF, also, the negative correlation in the gradient of MADT continues, while the meridional position of the STF and correlation appears to weaken.

There was no obvious relationship between the SAF and the SAM, other than if the data was smoothed with a 5-month running mean and an 18-month lag, when there was a correlation of -0.27 with a significance above the 95% confidence level in the meridional position. The gradient of MADT in the SAF while following the meridional position during the positive anomalies does not follow the meridional position throughout the time-series (see Table 2.). A strong correlation was found in the

gradient of MADT and the SAM (0.47 with a significance greater than 99%), however, the gradient of MADT then precedes a change in the SAM by 8-months. If the same lag is taken as the position, the correlation in the gradient of MADT against the SAM is -0.14, yet it is not significant.

Applying the 5-month running mean to the APF position and gradient of MADT resulted in negative correlation with the SAM, nonetheless, this is only after applying a 15-month lag to the data. Without applying a running mean to the monthly data or using a lag no significant relationships were found.

The SACCF did display a negative relationship with the SAM in both its meridional position and gradient of MADT in the monthly data with no lag, suggesting that part of the variability in the position and strength of the SACCF can be explained by the phase of the SAM. The correlation was performed and different lead/lags were investigated but there was no significant correlation. None of the correlations between the SBdy and the SAM were found to be significant, whether a running mean was applied or not.

The possible influence of the ENSO on the variability of the fronts along the Greenwich Meridian was investigated. No significant relationship was found between the meridional position and ENSO or the gradient of MADT at the frontal position and ENSO. Only the corrected STF frontal position showed a possible relationship to the ENSO, with no running mean, the STF position correlated with ENSO at 0.27 (significance greater than 99%), this was found by introducing a 12-month lag in the frontal position. Without the lag a relationship was still found in the STF and ENSO, however, the relationship becomes out of phase, -0.23 (significance greater than 95%).

Table 3. Correlations of the normalised frontal positions of the ACC at the Greenwich Meridian against the SAM

Frontal normalised meridional positions	SAM (significance)	Lag (months)	Correlation with lag removed (significance)	Correlation with no lag or running mean (significance)
STF	0.32 (<95%)	33	0.30 (<95%)	0.16 (<95%)
SAF	-0.26 (>95%)	18	-0.04 (<95%)	-0.08 (<95%)
APF	-0.41 (>95%)	15	-0.13 (<95%)	-0.13 (<95%)
SACCF	0.33 (<95%)	59	-0.19 (<95%)	-0.27 (>99%)
SBdy	0.33 (<95%)	48	0.01 (<95%)	-0.03 (<95%)

All correlation unless otherwise stated, like those in the last column are found using a 5-month running mean in all the data.

Table 4. Correlations of the normalised frontal gradients of MADT of the ACC at the Greenwich Meridian against the SAM

Frontal normalised gradient of MADT	SAM (significance)	Lag (months)	Correlation with lag removed (significance)	Correlation with no lag or running mean (significance)
STF	-0.33 (<95%)	19	-0.19 (<95%)	-0.11 (<95%)
SAF	0.47 (>99%)	-8	0.02 (<95%)	-0.09 (<95%)
APF	-0.36 (>95%)	15	-0.12 (<95%)	-0.11 (<95%)
SACCF	0.30 (<95%)	58	-0.18 (<95%)	-0.23 (>95%)
SBdy	-0.28 (<95%)	48	0.04 (<95%)	0.12 (<95%)

All correlation unless otherwise stated, like those in the last column are found using a 5-month running mean in all the data.

The mean monthly Microwave Optimally Interpolated SST used in this study is over the period from June 2002 – November 2007. The Integrated SST or the meridional sum of SST between the boundaries of each zone within the ACC at the Greenwich

Meridian is calculated. This provided a means of describing some of the surface variability within the individual zones of the ACC along the Greenwich Meridian. Due to the obvious relationship in the integrated SST values and distance between fronts, the integrated SST is divided by the distance between the northern and southern front of each zone. Each cell is equally spaced at 0.25°. Additionally, The high seasonality in the SST is removed so that the underlying interannual variability could be identified (see Figure 9). Using the corrected meridional positions of the fronts along the Greenwich Meridian the zones between the main frontal features are defined. The seasonal changes in SST show no semiannual cycle (not shown), all zones show a seasonal maximum (minimum) in March (October), though the seasonal cycles are prominent. By combining these techniques it is possible to remove much of the internal variability within the zones of the ACC. The remaining variability of the integrated SST could then be investigated.

The Subantarctic Zone (SAZ), Antarctic Polar Zone (APZ) and Southern ACC Zone (SACCZ) show prevalent increases in their mean zonal SST for approximately a year between 2006 and 2007. The SAZ mean SST increase more rapidly than the APZ to begin with, while the SACCZ peaks before both SAZ and APZ. The warm event of the SACCZ is shorter lived than those of the SAZ and APZ (Figure 9a, b, c). A warming trend is apparent in the SAZ over the 2002 to 2007 time-series, while there appears to be a cooling trend in the SBZ.

A 2-month running mean needed to be added to the data of the SAZ before stronger correlations with the SAM were found. Notwithstanding the two most southern zones, the SACCZ and the SBZ, these display negative correlations with the SAM, -0.27 (significance above 99%) and -0.24 (significant above 95%) respectively without a

running mean (see Table 5). With a 2-month running mean applied, the correlations with zero lags are no longer significant above 95%. However, the SAZ, SACCZ, and SBZ show more pronounced correlations when lags are considered. Possible mechanisms for lag will be discussed in the next section. When considering the ENSO, no relationship is found with significance except for the SACCZ and SBZ with a 6-month ($r = 0.29$ >95%) and 24-month ($r = 0.33$ >99%) lag respectively. This is in agreement with Sallée *et al.* (2008) who noted that the ENSO outside of the Pacific basin tends to be anticorrelated with the SAM response.

(a)

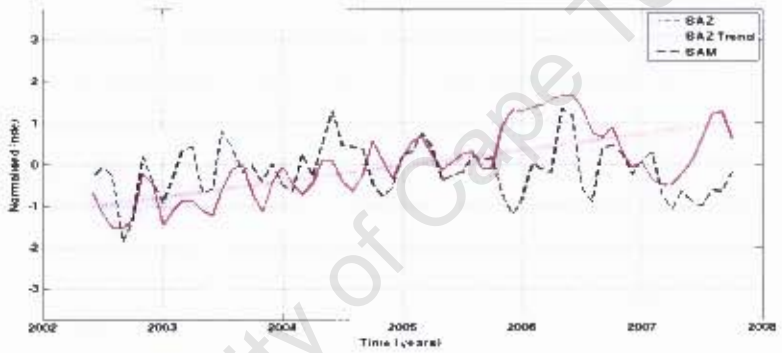

(b)

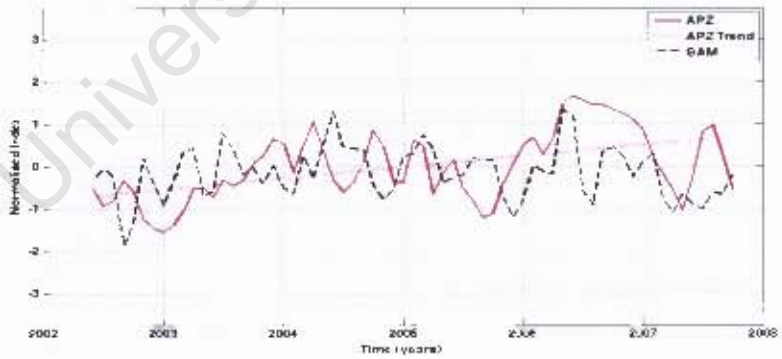

Figure 9. Plots of the normalised index of mean SST (°C/0.25° latitude) with a 2-month running mean through each zone with the mean seasonal cycles removed. This is illustrated for (a) The SAZ, (b) the APZ, (c) the SACCZ, (d) the SBZ. Plotted against the SAM, also with a 2-month running mean applied to its index.

(c)

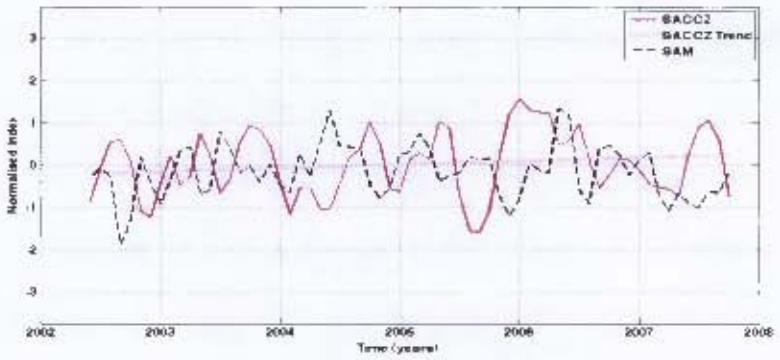

(d)

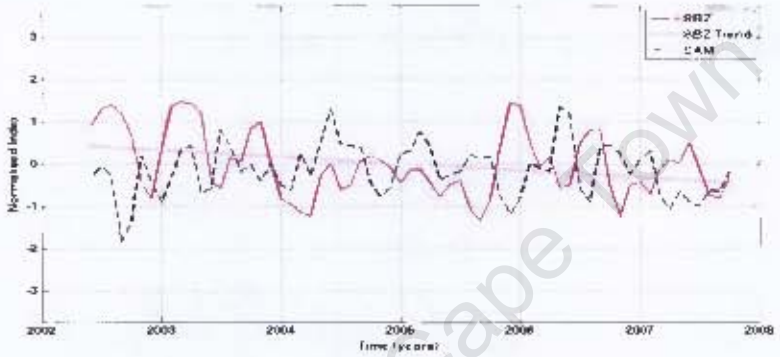

Figure 9. Plots of the normalised index of mean SST (^{0}C/0.25^{0} latitude) with a 2-month running mean through each zone with the mean seasonal cycles removed. This is illustrated for (a) The SAZ, (b) the APZ, (c) the SACCZ, (d) the SBZ. Plotted against the SAM, also with a 2-month running mean applied to its index.

When examining Figure 9 it becomes apparent that there is a change in the integrated SST. With latitude from north to south there is a change from a strong positive trend in SST in the SAZ to a strong negative trend in the integrated SST in SBZ.

It should be noted that the SAM index used in this study from 1993 to 2007 shows a slight negative trend. Nonetheless, the SAM has shown a positive trend over recent decades and has been in an anomalously positive phase throughout the majority of the study period, consequently much of the correlations of the remotely sensed data with the SAM are during an already positive phase in the SAM.

Table 5. Correlations of normalised mean integrated SST for the zones of the ACC along the Greenwich Meridian against the SAM

Zonal Integrated SST	SAM with 2-month running mean & lag considered	Lag	SAM without a running mean or lag
SAZ	--0.28 (>95%)	13	0.16 (<95%)
APZ	0.23 (<95%)	3	0.08 (<95%)
SACCZ	-0.32 (>95%)	14	-0.27 (>99%)
SBZ	0.40 (>95%)	23	-0.24 (>95%)

The potential mechanisms associated with the observed trends in the meridional positions and gradient of MADT of the fronts will be discussed in the section.

4. Discussion

4.1 Variability in the Fronts of the ACC along the Greenwich Meridian

The disturbances in the STF where corrections in the meridional frontal position were made were found to be due to mesoscale features being tracked, rather than the true meridional frontal position. The STF is known have a highly variable spatial structure due to the meandering in the STF and mesoscale eddies (Belkin & Gordon, 1996; Swart *et al.* 2008). Nonetheless, it is not clear if these disturbances are due to the Agulhas Ring Corridor being located further south from its mean position, alternatively increased meandering of the STF might be causing additional mixing of the SASW and subtropical surface waters. The example in Figure 5 and the other anomalous periods identify limitations in the use of MADT as a means of locating and following frontal features in both time and space, in regions of intense mesoscale variability. An intriguing observation, however, is that the same periods of anomalous activity in the STF coincide with positive phases of the SAM (see Figure 1 & Figure 4a). These are not single events but rather anomalous periods of a year or longer

when Agulhas Rings interact with the STF at the Greenwich Meridian. Whether this is a coincidence, or whether mechanisms associated with the SAM are forcing the STF to branch and meander was not investigated. It is possible that the phase of the SAM can influence the interannual variability of spawning mesoscale eddies at the Agulhas Current Retroflection. Little has been done in this field, due to the difficulty in tracking Agulhas Rings using observational data. Agulhas Rings decay over time and therefore their signature is constantly changing. Using SST is not always appropriate since the skin temperature of the eddy may be the same as the surrounding waters while the ring is still present. The use of altimetry also struggles to follow and capture individual eddies when temporal coverage is limited, eddy tracks can vary and merge, and the sea level anomaly signals of the eddies weaken in time.

4.1.1 Seasonal Variability

The seasonality of the STF, SACCF and SBdy meridional positions are particularly noticeable. The seasonal variability in the meridional positions displays a reasonable response. Cooling of the ocean occurs during the winter, and therefore a northward migration in the MADT isolines occurs due to a steric change in seawater in the upper ocean. The meridional migrations of the frontal positions in the southern sector of the ACC are largely uniform. Both the SACCF and SBdy meridional mean seasonal shifts share similar characteristics. The more southerly of the two, the SBdy, leads the SACCF by approximately one month, also the magnitude of the seasonal variability of the SBdy is greater than that of the SACCF. The most southerly seasonal position is found in October (SBdy) and November (SACCF). This is a period of change in the Southern Ocean when the austral winter has come to and end and austral summer is beginning to dominate. A small second peak in both the SBdy (May) and SACCF (June) occurs at a period when the Southern

Hemisphere is entering winter. A reason for this might be the slow oceanic response to solar heating during the austral summer, and the high thermal heat capacity of seawater. SAF & APF show weak seasonal variability in their meridional frontal positions. This is likely due to the high uv velocity magnitudes found in the SAF and APF, which are created through pronounced gradients in density.

Previous studies have found that the seasonal cycle in the mid and high latitudes of the Southern Hemisphere have changed in recent decades (Rouault *et al.* 2005). The seasonal changes can be attributed to documented changes in the Semiannual Oscillation (SAO). The SAO has under gone changes since the 1960's (Rouault *et al.* 2005). These changes in the SAO have been linked to changes in the polar vortex, which are largely due to photochemical ozone depletion (Thompson & Solomon, 2002). The SAO displays a twice-yearly intensification in the midtropospheric thermal gradient between 50° – 65°S (Rouault *et al.* 2005), which is situated directly over the southern sector of the ACC. It is likely that the mean seasonal cycles applied to the data do not accurately represent the seasonal changes through the time-series due to changes in the SAO from 1993 to 2007.

4.1.2 Interannual Variability and Connection between Meridional Position and Gradient of MADT

The interesting question raised here is why the meridional positions of the fronts in the ACC shift northward (southward) in conjunction with a strengthening (weakening) in the gradient of MADT, and why this relationship is reversed in the SBdy (see Table 2). A possible explanation might be that the frontal positions are created through the convergence of differing water masses. If there is an anomalous amount of cool water advecting northward, the gradient between the northward advecting water and

the warmer southward advecting water will be intensified. A cool water event would result in an increased gradient in the front and a northward shift in the meridional position of the front. If, on the other hand, there is an anomalous southward shift in warmer water, one would also expect the gradient to increase, but with a southward migration in the meridional frontal position. Cool northward advecting water is a dominant feature of the ACC and is present at all times in the ACC (Belkin & Gordon, 1996), it is therefore unlikely that even an increased southward flow of water from the north would force the frontal positions south, while anomalous northward flow would further dominate the forcing of the meridional position and cause a northward shift, along with an increase in the gradient of MADT at the front.

It must be stressed that this study has not investigated possible mechanisms responsible for these results. Further studies are required to investigate whether changes in the Sea Level Pressure (SLP), wind stress, wind stress curl, and heat fluxes at mid and high latitudes can help explain the variability observed in the meridional position and gradient of MADT in the fronts of the ACC at the Greenwich Meridian.

4.2 The Southern Annular Mode and Southern Ocean frontal variability

With the mean seasonal cycles removed from the fronts within the ACC at the Greenwich Meridian pronounced interannual variability persists. As shown in Table 2, the gradient of MADT in the fronts is closely linked to the meridional position of the fronts. The strength in the gradient of MADT at the fronts is an indicator to the degree of change in density from one water mass to the next on opposing sides of the fronts. Additionally, the intensity of convergence-divergence of upper ocean waters is likely to influence the strength in gradient of MADT. A product of such changes will

undoubtedly influence the meridional position. Dynamic and thermodynamic responses through surface stresses and alteration of the heat and freshwater fluxes, are capable of changing the upper ocean characteristics (Sen Gupta & England, 2006). Changes in the westerly winds are associated with changes in the phase of the SAM. Changes in the SAM are therefore likely to change the dynamic and thermodynamic relationship between the ocean-atmosphere system in the Southern Ocean.

The mid and upper layers of the Southern Ocean have shown a warming trend in recent decades, with the observed warming concentrated in the ACC between 45° – 60°S (Gille, 2002). Cooling (warming) trends to the north (south) of 1.3 dyn m in the ACC have been documented (Gille, 2002). The long-term trends in the meridional frontal positions of the ACC along the Greenwich Meridian have remained static or shown a southward migration over the 15-year time-series (STF, SACCF, SBdy). A southward migration of the SACCF and SBdy supports the findings by Gille (2002) that warming has occurred south of the 1.3 dyn m contour. North of the 1.3 dyn m contour is the APZ, the APF on the northern boundary of the APZ has shown a northward migration in its meridional positions, indicating a cooling. This would also support Gille (2002), which may be attributed to increased divergence from the south and subduction of colder waters at the APF. The southward shift in the meridional position of the STF may be related to the decrease in westerly winds and a southward shift in subtropical waters as noted by Cai (2006). A warming of the upper and mid ocean layers is associated with a change in density of the seawater, which should be expressed in a southward drift in the contours of dynamic height. Gille (2002) noted that warming was found in the subducting SASW, sometimes referred to as the Subantarctic Mode Water. SASW is situated at the surface between the

SAF and the STF, which is referred to as the SAZ in this study. The SST signature of the SASW in the SAZ has shown a considerable warming since 2002 (Figure 10a) with a weak positive correlation (r = 0.16) with the SAM, although it is not significant above the 95% confidence level. Despite the weak correlation, it does at least suggest that the SAZ favours warming during a positive SAM. The cooling of SST in the southern zones of the ACC along the Greenwich Meridian can potentially be explained by the southward shift and increased strength of westerly winds. A southward shift and strengthening of the westerly winds are associated with a positive phase in the SAM. Correlations between the Integrated SST of the SACCZ and SBZ with SAM show a negative response with no lag or running mean applied. The response of SST in the southern ACC is to cool, this is arguably due to the combination of anomalous heat fluxes and enhanced Ekman transport. The meridional positions may still move south as the warming in the southern sector is in the mid and upper layer of the Southern Ocean and therefore not in direct contact with the surface.

The results in the SST data from the this study support the numerical modelling work conducted by Sen Gupta & England (2006) which imply that increased northward Ekman transport occurs at around 60°S, while an easterly intensification of winds at approximately 40°S causes a poleward response in Ekman transport. This is indicated by the immediate warming of SST in the SAZ and cooling in the SACCZ and SBZ. The changes in the Ekman transports during positive phases in the SAM are associated with weak westerlies and easterly winds at approximately 35° – 40°S and strong westerly winds between 55° – 60°S (Sen Gupta & England, 2006; Sallée *et al.* 2008).

Reduced winds and increased SLP over the SAZ are likely to favour warmer SST. SST is, however, sensitive to rapid changes in the atmosphere. Transient eddies and synoptic features can rapidly alter SST in zones of the ACC. Furthermore, despite the long term trend of the SACCF and SBdy meridional positions, when correlated against the SAM, they do not show significant relationships. An identifiable problem with using MADT to locate the meridional frontal positions and to then identify a relationship with an atmospheric mode is extremely difficult. The SAM oscillates on all timescale from synoptic to centennial (Hall & Visbeck, 2002), at which temporal scales does the ACC respond to forcing from the SAM. This is made more difficult by the fact that the current use of MADT limits studies to interannual and annual timescales. Moreover, the response of the ACC to the SAM is likely to vary with depth, with the upper ocean responding quicker. This might be why the Microwave Optimally Interpolated SST data has shown a clearer relationship with the SAM despite its shorter time-series. The SAM has shown a positive trend since the 1970's (Thompson & Solomon, 2002), which might explain the longer-term trends in the meridional positions and gradients of MADT.

The SBZ displays an immediate cooling of SST against the SAM when it is in a positive phase. However, when a lag is added the SBZ SST increases under a positive SAM. The lag is considerable, at 23-months, which is questionable when the time-series has only 64-months of data when using a 2-month running mean. Meredith & Hogg (2006) found anomalous Eddy Kinetic Energy (EKE) in the ACC during the 2000 – 2002 period and attributed this to a positive phase of the SAM during 1998. Using an eddy-resolving model Meredith & Hogg (2006) established that increasing westerly winds are associated with a delayed increase in eddy activity. Consequently, if Meredith & Hogg (2006) are correct, the documented

changes in the SAM in recent decades (Thompson & Solomon, 2002) might help further explain the observed warming in the ACC (Gille, 2002) by increasing poleward heat fluxes. While the 23-month lag of SST in the SBZ is a possible indicator to warming through increased eddy activity, the meridional positions of the SACCF and SBdy, both show a correlation with the SAM, which is positive (<95%) with over a 4-year lag. This is in contrast to the findings by Meredith & Hogg (2006) who associated a warming in the southern sector of the ACC with a positive SAM. Although, increased eddy activity may in fact act to transport cool waters northward and cool the southern sector on interannual timescales. In addition, the 4-year lag can possibly be elucidated by the findings of Meredith & Hogg (2006) who stated that eddy activity in response to the SAM takes approximately 4-years to return to a steady state. Nevertheless, the length of the lag makes this result contentious until a longer time-series is available or alternative methods are used to further investigate the relationship in the SAM and meridional positions of the SACCF and SBdy.

The SAF and APF do express negative correlations in their meridional position with the SAM with an 18-month ($r = -0.26$) and 15-month ($r = -0.41$) lag respectively, both correlations are significant above the 95% confidence level. This does indicate a warming in the fronts in relation to the SAM with a lag of over a year. Sen Gupta & England (2006) noted an increased Ekman convergence and downwelling at 45° – 55°S in their simulated response of the ACC during a positive SAM forcing. An indicator of increased convergence is the gradient of MADT at a frontal position. The gradient of MADT in the SAF (~45°S) did show a strong positive correlation with the SAM ($r = 0.47$ >99%), however, the change in the gradient of MADT precedes the SAM by eight months. This is an unexpected finding with no explanation available at this time. The gradient response of MADT did not show a clear relationship with the

SAM. Correlations are either negative (APF), which do not correspond with the simulated model response found by Sen Gupta & England (2006) or the correlations lag considerably and are not significant above 95% confidence level. The gradient of MADT and meridional position of the APF has, however, shifted northward and intensified. This finding supports Sen Gupta & England (2006) in as far as supporting their conclusions of increased Ekman transport and downwelling at the latitude near the APF, although only a weak correlation was found. An important difference in the coupled numerical model studies of the SAM and its influence on the ACC and those of MADT is that the model response of the horizontal ocean circulation to the SAM is restricted to the surface, while the MADT takes into account the entire water column. Nonetheless, further studies should be carried out to investigate the delayed responses in the fronts due changes in the SAM.

The zonal wind component is only one part of the surface expression. Meridional winds contribute significantly to the state of the ACC, moreover, synoptic scale features are capable of changing the phase of the SAM (Meehl *et al.* 2001). The numerical studies on the response of the ACC to the SAM conducted to date (Hall & Visbeck, 2002; Sen Gupta & England, 2006) do not take into account mesoscale features. This is a fundamental limitation in such studies, as eddies are thought to contribute a significant amount to meridional heat fluxes in both the atmosphere and ocean (Meredith & Hogg, 2006). Despite the limitations of the numerical models, they do capture the oceanic response reasonably well. Of course regional differences and responses are considerable (Sallée *et al.* 2008) and not fully represented in the coupled numerical models. Further observational studies are required to better resolve the fundamental dynamics that drive variability in the ACC.

4.3 Frontal Zones of the ACC along the Greenwich Meridian and the El Niño–Southern Oscillation

The correlation of the meridional position of the STF and the ENSO is 0.27 with a lag of 12 months. This supports Colberg *et al.* (2004) who used a general circulation model to model the response of the South Atlantic to the ENSO. Their model suggested that El Niño should cause an increase in the northward Ekman drift through an increase in the midlatitude westerlies, which were found to increase under El Niño through a strengthening of the South Atlantic subtropical anticyclone. A positive wind stress curl over the SASW would be expected to force the STF northward, the opposite being true for a La Niña event. The integrated SST data for the SAZ showed a cooling under a positive ENSO, although the correlation is weak. The correlations of the SACCZ and SBZ against the ENSO both showed positive relationships, 0.29 (>95%) and 0.33 (>99%) respectively. The SACCZ lagged ENSO by 6-months, while the SBZ lagged by 24-months, given the length of the time-series, lags this length make the results questionable at best. Having said that, the results indicate under El Niño (La Niña), integrated SST in the southern sector of the ACC is more likely to be warming (cooling).

Despite the models findings and observational agreements, caution must be applied as the model also suggested that the response in the South Atlantic to the ENSO is non linear. Sallée *et al.* (2008) found that the ENSO has a lower frequency response on SST in the ACC than the SAM. The lower frequencies of integrated SST, did show better correlations, however, the length of available Microwave Optimally Interpolated SST data does not favour such studies, yet.

5. Summary

Until recently previous studies have been limited by the amount of available data, with the harsh environment of the Southern Ocean being a major obstacle. Recent developments in the use of altimetry data have made it possible to accurately map the MADT of the ocean in great detail.

A good agreement between the altimetry derived meridional positions of the ACC along the Greenwich Meridian with those found by Orsi *et al.* (1995) using hydrographic data was found. This confirms that the use of altimetry along the Greenwich Meridian is a robust method in identifying the frontal features, although caution should be used in the northern sector of the ACC as mesoscale features can cause inaccuracies in the method.

There appears to be stronger seasonal features at the northern and southern boundaries of the ACC, while the central fronts showed less seasonality. An interesting observation was that the gradient of MADT of the frontal feature is directly related to its meridional position. There was a strong positive correlation between the meridional position of the SAF, APF and SACCF and their gradients. The SBdy, showed a strong negative correlation in its meridional position and gradient of MADT. The relationship between the meridional position of the STF and its gradient of MADT remained somewhat ambiguous.

The study found that the values of MADT used as a contour through time along the Greenwich Meridian have not remained stationary, and have instead shown migratory trends. All frontal meridional positions have shifted south from the period of

1993 to 2007, except for the APF, which has moved northward. These findings support Gille (2002) that the Southern Ocean appears to be warming (cooling in the APZ zone) and possibly freshening south of 55°S (Wong *et al.* 1999).

The integrated SST in the zones between the fronts along the Greenwich Meridian also exhibits trends over the period of observation. From north to south, the zones show a steady change in their integrated SST. The most northern zone, the SAZ shows the greatest warming (°C/0.25° latitude) with a steady decline in each zone further south. The SBZ, the zone furthest south, exhibits a cooling trend over the observed period. This would also support the coupled ocean-atmosphere studies (Hall & Visbeck, 2002; Sen Gupta & England, 2006) that the intensifying and southward migration of the westerly winds might be changing the Ekman transports in the upper ocean of the ACC as well changing the heat fluxes and other variables associated with ocean-atmospheric feedbacks.

The interannual variability of the meridional positions and gradient of MADT did display weak relationships with the SAM, however, the results are far from conclusive. Reasons for this might be that the interannual variability of the ACC is likely to be dominated by the overlying atmosphere in only the upper ocean and the MADT takes the entire water column into account, furthermore, the slow oceanic response to changes in the overlying atmosphere may be masking the response. Still, integrated SST displayed features suggesting a relationship with the SAM, yet the correlations also remained weak. It must be emphasised that the study periods ran from 1993 to 2007, during this time, the SAM remained in an anomalously positive phase in comparison to previous decades, therefore interannual responses to the same may be hidden under the already anomalously high phase of the SAM.

The dynamics are clearly more complex and cannot be fully explained by the SAM alone. Longer time-series of the data, as well as further investigation into the mechanisms using a combination of reanalysis data, model data and observational data are needed to establish why the fronts are changing and why there is interannual variability present.

A regional snapshot, such as this study is likely to be dominated by regional forcings as found by Sallée *et al.* (2008) and mesoscale activity, which are not reflected in the SAM. Nonetheless, this study provides some confidence for coupled ocean-atmosphere models using relatively coarse resolutions to capture the main features in the ocean-atmosphere system of the Southern Ocean and the overlying atmosphere. In addition, altimetry data has proved to be an indispensable method in observing the interannual variability of the ACC fronts along the Greenwich Meridian, nevertheless, further studies are required to explain the observed variability.

Acknowledgements

Sincere thanks must go to Sebastiaan Swart for his indispensable help and support in this project. The invaluable support and input from Professor Chris Reason and Dr Juliet Hermes is greatly appreciated, as well as all the help received from postgraduate students in the department, noticeably Neil Hart and Natalie Burls. The work presented here is support by the centre for High Performance Computing (CHPC) through the provision of funds. Dr Gareth Marshall at the British Antarctic Survey & Dr Klaus Wolter at NOAA are thanked for their provision of the SAM index (http://www.antarctica.ac.uk/met/gjma/sam.html) and the MEI index (http://www.cdc.noaa.gov/people/klaus.wolter/MEI/) respectively, for the Earth Science community. The altimeter products were produced and distributed by Aviso, as part of the Ssalto ground processing segment. Microwave Optimally Interpolated SST data are produced by Remote Sensing Systems and sponsored by National Oceanographic Partnership Program (NOPP), the NASA Earth Science Physical Oceanography Program, and the NASA REASON DISCOVER Project. Data are available at www.remss.com.

References

Belkin, I. M., Gordon, A. L., 1996: Southern Ocean fronts from the Greenwich meridian to Tasmania. Journal of Geophysical Research, Vol. 101, No. C2, pp3675-3696

Burls, N. J., Reason, C. J. C., 2006: Sea surface temperature in the midlatitude South Atlantic by using microwave satellite data. Journal of Geophysical Research, Vol. 111, C08001, DOI:10.1029/2005JC003133

Cai, W., 2006: Antarctic ozone depletion causes an intensification of the Southern Ocean super-gyre circulation. Geophysical Research Letters, Vol. 33, L03712, doi:10.1029/2005GL024911

Colberg, F., Reason, C. J. C., Rodgers, K., 2004: South Atlantic response to El Niño – Southern Oscillation induced climate variability in an ocean general circulation model. Journal of Geophysical Research, Vol. 109, C12015, DOI:10.1029/2004JC002301

Ducet, N., Le Traon, P. Y., Reverdin, G., 2000: Global high-resolution mapping of ocean circulation from TOPEX/Poseidon and ERS-1 and -2. Journal of Geophysical Research, Vol. 105, pp19,477-19,498

Gille, S. T., 2002: Warming of the Southern Ocean Since the 1950s. Science, Vol, 296, pp1275-1277, DOI: 10.1126/science.1065863

Gong, D., Wang, A., 1999: A Definition of the Antarctic Oscillation Index. Geophysical Research Letters, Vol. 24, pp459-462

Gordon, A. L., 1986: Interocean Exchange of Thermocline Water. Journal of Geophysical Research, Vol. 91, No. C4, pp5037-5046

Hall, A., Visbeck, M., 2002: Synchronous Variability in the Southern Hemisphere Atmosphere, Sea Ice, and Ocean Resulting form the Annular Mode. Journal of Climate, Vol. 15, pp3043-3057

Hines, K., Bromwich, D., Marshall, G., 2000: Artificial Surface Pressure Trends in the NCEP-NCAR Reanalysis over the Southern Ocean and Antarctica. Journal of Climate, Vol. 13, pp3940-3952

Marshall, G. J., 2003: Trends in the Southern Annular Mode from observations and reanalyses. Journal of Climate, Vol 16, Issue 24, pp4134-4143

Meehl, G. A., 1991: A Re-examination of the Mechanism of the Semiannual Oscillation in the Southern Hemisphere. Journal of Climate, Vol. 4, Issue 9, pp911-926, DOI: 10.1175/1520-0442(1991)004<0911:AROTMO>2.0.CO;2

Meehl, G. A., Lukas, R., Kiladis, G. N., Weickmann, K. M., Matthews, A. J., Wheeler, M., 2001: A conceptual framework for time and space scale interactions in the climate system. Climate Dynamics, Vol. 17, pp753-775

Meredith, M. P., Hogg, A. M., 2006: Circumpolar response of Southern Ocean eddy activity to a change in the Southern Annular Mode. Geophysical Research Letters, Vol. 33, L16608, DOI:10.1029/2006GL026499

Mo, K. C., 2000: Relationships between Low-Frequency Variability in the Southern Hemisphere and Sea Surface Temperature Anomalies. Journal of Climate, Vol. 13, Issue 20, pp3599-3610, DOI: 10.1175/1520-0442(2000)013<3599:RBLFVI>2.0.CO;2

Moore, J. K., Abbott, M. R., Richman, J. G., 1997: Variability in the location of the Antarctic Polar Front (90° – 20°W) from satellite sea surface temperature data. Journal of Geophysical Research, Vol. 102, No. C13, pp27,825-27,833

Moore, J. K., Abbott, M. R., Richman, J. G., 1999: Location and dynamics of the Antarctic Polar Front from satellite sea surface temperature data. Journal of Geophysical Research, Vol. 104, No. C2, pp3059-3073

Orsi, A., Whitworth, T., Nowlin, W. D., 1995: Om the meridional extent and fronts of the Antarctic Circumpolar Current. Deep-Sea Research Part 1: Oceanographic Research Papers, Vol. 42, Issue 5, pp641-673, doi:10.1016/0967-0637(95)00021-W

Le Traon, P. Y., Nadal, P. F., Ducet, N., 1998: An improved mapping method of multisatellite altimeter data. Journal of Atmospheric and Oceanic Technology, Vol. 15, issue 2, pp522-534, DOI: 10.1175/1520 0426(1998)015<0522:AIMMOM>2.0.CO;2

Le Traon, P. Y., Ogor, F., 1998: ERS-1/2 orbit improvement using TOPEX/POSEIDON: The 2cm challenge. Journal of Geophysical Research, Vol. 103, pp8045-8057

Lutjeharms, J. R. E., Valentine, H. R., 1988: Eddies at the Subtropical Convergence South of Africa. Journal of Physical Oceanography, Vol. 18, Issue 5, pp761-774, DOI: 10.1175/1520-0485(1988)018<0761:EATSCS>2.0.CO;2

Lutjeharms, J. R. E., Ansorge, I. J., 2001: The Agulhas Return Current. Journal of Marine Systems, Vol. 30, Issues 1-2, pp115-138, DOI:doi:10.1016/S0924-7963(01)00041-0

Reason, C. J. C., 2001: Evidence for the Influence of the Agulhas Current on Regional Atmospheric Circulation Patterns. Journal of Climate, Vol. 14, Issue 12, pp2769-2778, DOI: 10.1175/1520-0442(2001)014<2769:EFTIOT>2.0.CO;2

Reynolds, R. W., Smith, T. M., 1994: Improved Global Sea Surface Temperature Analyses Using Optimum Interpolation. Journal of Climate, Vol. 7, issue 6, pp929-948, DOI: 10.1175/1520-0442(1994)007<0929:IGSSTA>2.0.CO;2

Rintoul, S. R., 1991: South Atlantic interbasin exchange. Journal of Geophysical Research, Vol. 96, No. C2, pp2675-2692

Rio, M. H., Hernandez, F., 2004: A mean dynamic topography computed over the world ocean from altimetry, in-situ measurements, and a geoid model. Journal of Geophysical Research, Vol. 109, C12032, DOI:10.1029/2003JC002226

Rouault, M., Mélice, J-L., Reason, C. J. C., Lutjeharms, J. R. E., 2005: Climate variability at Mariona Island, Southern Ocean, since 1960. Journal of Geophysical Research, Vol. 110. C05007, DOI:10.1029/2004JC002492

Sallée, J. B., Speer, K., Morrow, R., 2008: Response of the Antarctic Circumpolar Current to Atmospheric Variability. Journal of Climate, Vol. 21, pp3020-3039, DOI:10.1175/2007JCLI1702.1

Sen Gupta, A., England, M. H., 2006: Coupled Ocean–Atmosphere–Ice Response to Variations in the Southern Annular Mode. Journal of Climate, Vol. 19, pp4457-4486

Sloyan, B. M., Rintoul, S. R., 2001a: The Southern Ocean Limb of the Global Deep Overturning Circulation. Journal of Physical Oceanography, Vol. 31, Issue 1, pp143-173

Sloyan, B. M., Rintoul, S. R., 2001b: Circulation, Renewal, and Modification of Antarctic Mode and Intermediate Water. Journal of Physical Oceanography, Vol. 31, Issue 4, pp1005-1030

Sokolov, S., Rintoul, S. R., 2007: Multiple jets of the Antarctic Circumpolar Current south of Australia. Journal of Physical Oceanography, Vol. 37, Issue 5, pp1394-1412

Speer, K., Rintoul, S. R., Sloyan, B., 2000: The Diabatic Deacon Cell. Journal of Physical Oceanography, Vol. 30, Issue 12, pp3212-3222

Speich, S., Blanke, B., Madec, G., 2001: Warm and cold water routes of an OGCM thermohaline Conveyor Belt. Geophysical Research Letters, Vol. 28, No. 2, pp311-314

Swart, S., Speich, S., Ansorge, I. J., Goni, G. J., Gladyshev, S., Lutjeharms, J. R. E., 2008: Transport and variability of the Antarctic Circumpolar Current south of Africa. Journal of Geophysical Research, Vol. 113, C09014, DOI:10.1029/2007JC004223

Swart, S., Speich, S., 2009 (In Press): An Altimetery-Based Gravest Empirical Mode South of Africa: Dynamic Nature of the Antarctic Circumpolar Current Fronts. Journal of Geophysical Research

Swart, S., Speich, S., Ansorge, I. J., Lutjeharms, J. R. E., 2009 (In Press): A Satellite Based Gravest Empirical Mode South of Africa: Development and Validation. Journal of Geophysical Research

Thompson, D. W. J., Wallace, J. M., 2000: Annular Modes in the Extratropical Circulation. Part I: Month-to-Month Variability. Journal of Climate, Vol. 13, Issue 5, pp1000-1016

Thompson, D. W. J., Solomon, S., 2002: Interpretation of recent Southern Hemisphere climate change. Science, Vol 296, pp895-899

Trenberth K. E., W. G. Large and J. G. Olson (1990) The mean annual cycle in global ocean wind stress. Journal of Physical Oceanography, Vol 30, pp1742-1760.

Van Loon, H., 1967: The Half-Yearly Oscillations in Middle and High Southern Latitudes and the Coreless Winter. Journal of the Atmospheric Sciences, Vol. 24, Issue 5, pp472-486, DOI: 10.1175/1520-0469(1967)024<0472:THYOIM>2.0.CO;2

White, W. B., Peterson, R. G., 1996: An Antarctic Circumpolar Wave in Surface Pressure, Wind, Temperature and Sea-Ice extent. Nature, Vol. 380, pp699 - 702

Witter, D. L., Gordon, A. L., 1999:Interannual variability of South Atlantic circulation from 4 years of TOPEX/POSEIDON satellite altimeter observations. Journal of Geophysical Research, Vol 104(C9), pp20927-20948

Wolter, K., Timlin, M. S., 1993: Monitoring ENSO in COADS with a seasonality adjusted principal component index. Proc. of the 17th Climate Diagnostics Workshop, Norman, OK, NOAA/NMC/CAC, NSSL, Oklahoma Clim. Survey, CIMMS and the School of Meteor., Univ. of Oklahoma, 52-57

Wolter, K., Timlin, M. S., 1998: Measuring the strength of ENSO events - how does 1997/98 rank? Weather, 53, 315-324

Wong, A. P. S., Bindoff, N. L., Church, J. A., 1999: Large-scale freshening of intermediate waters in the Pacific and Indian Oceans. Nature, Vol. 400, pp440-443

Appendix

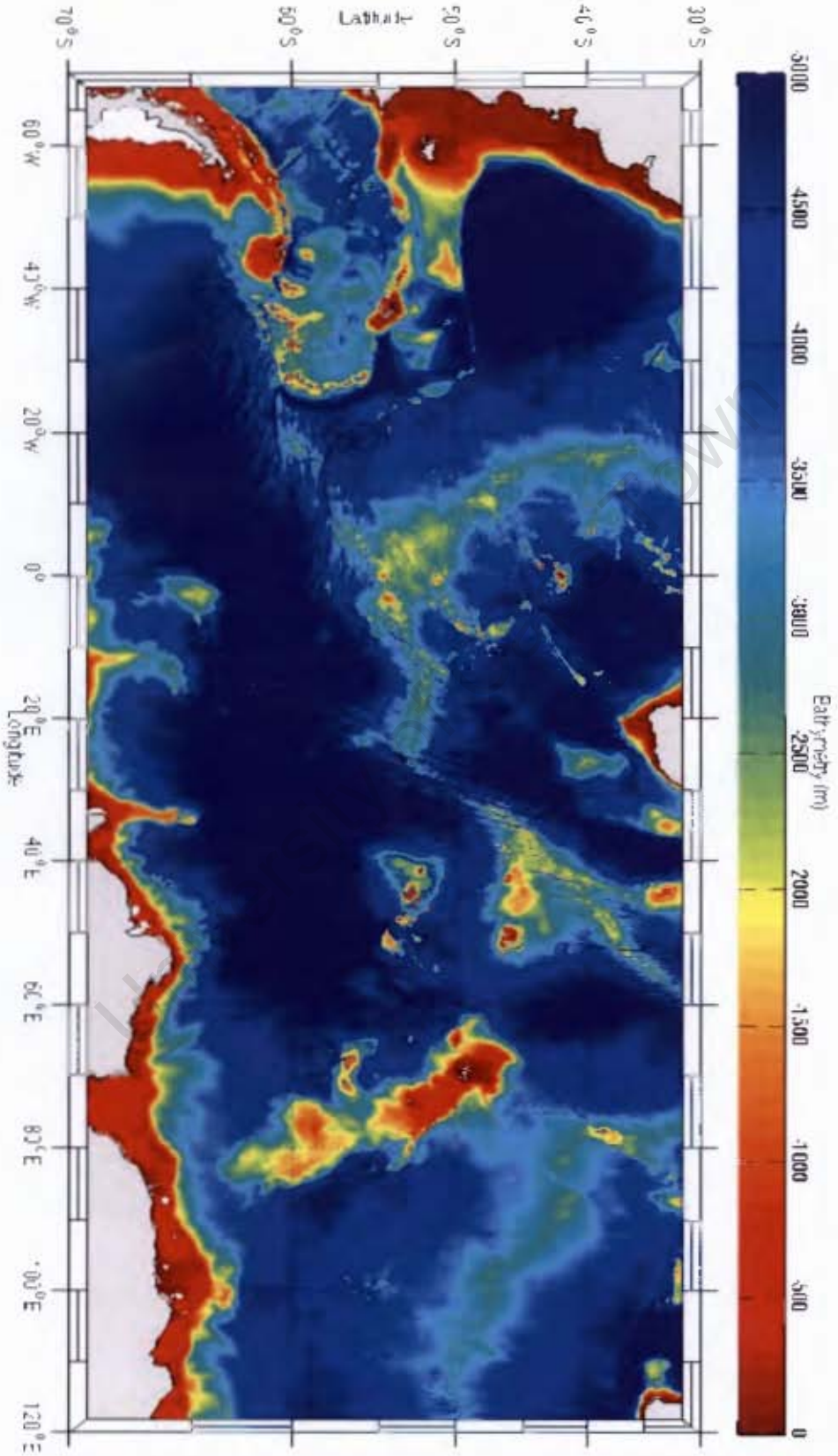

Figure 10. A bathymetric map (m) of the Southern Ocean from -60W – 120°E